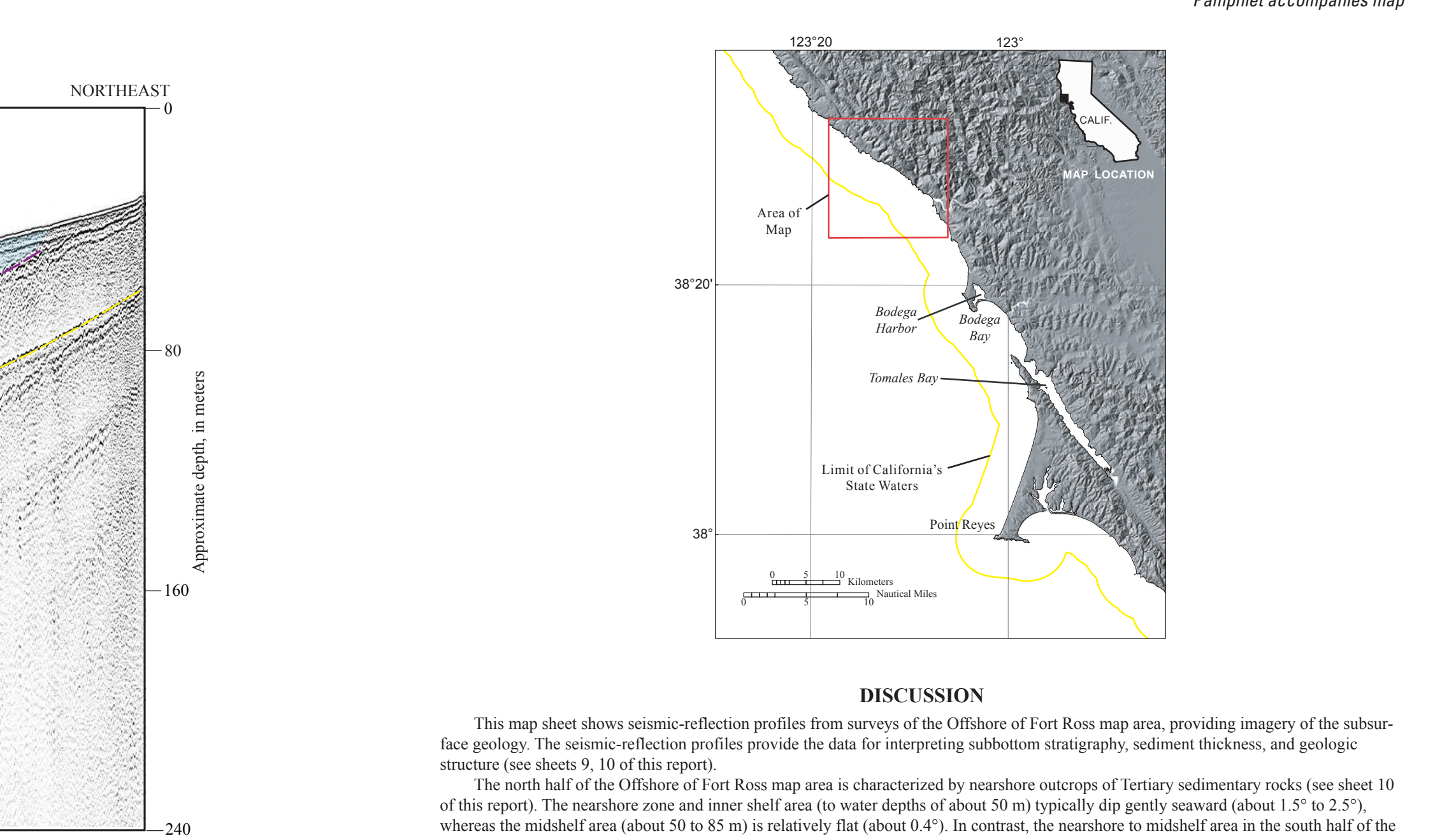
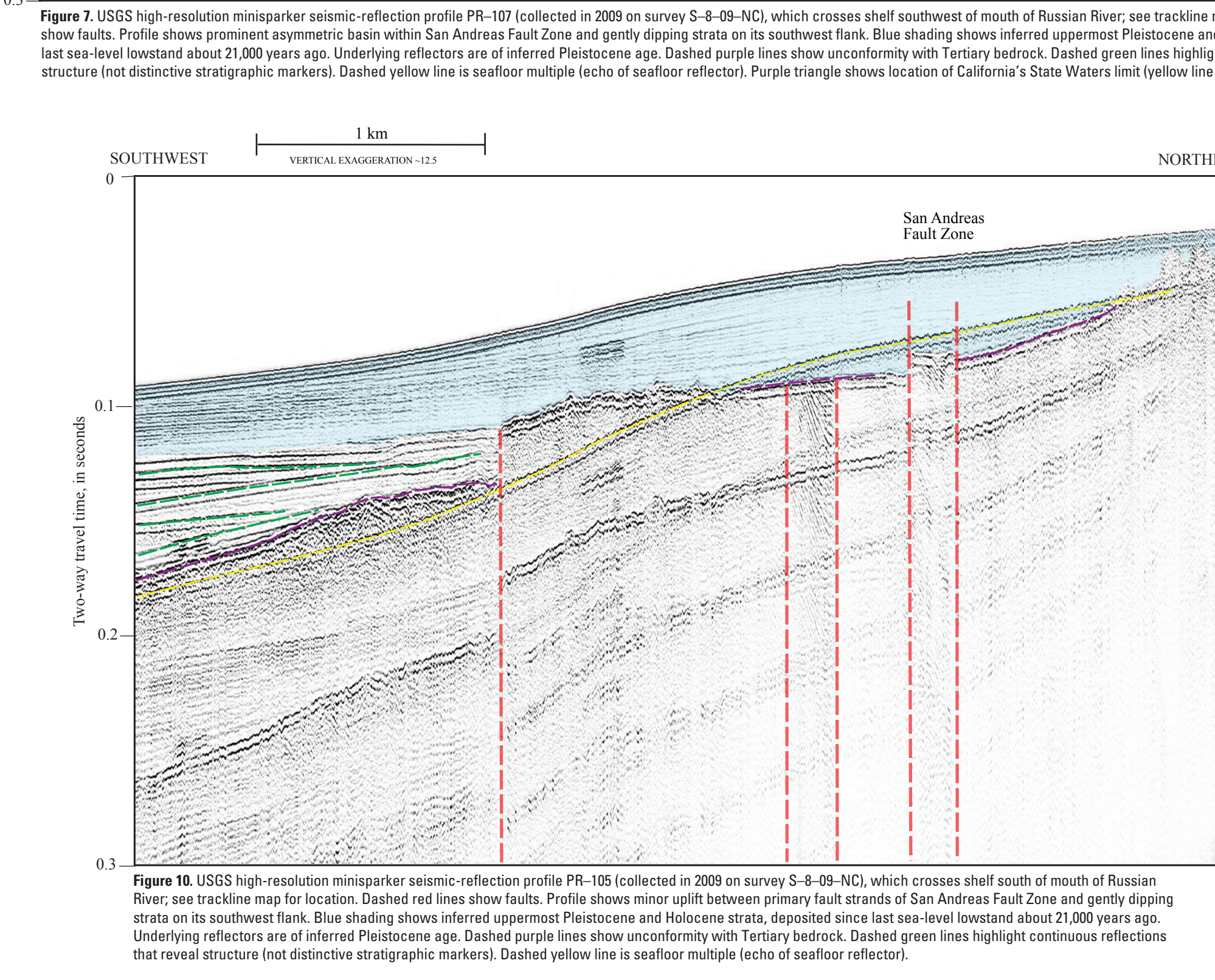
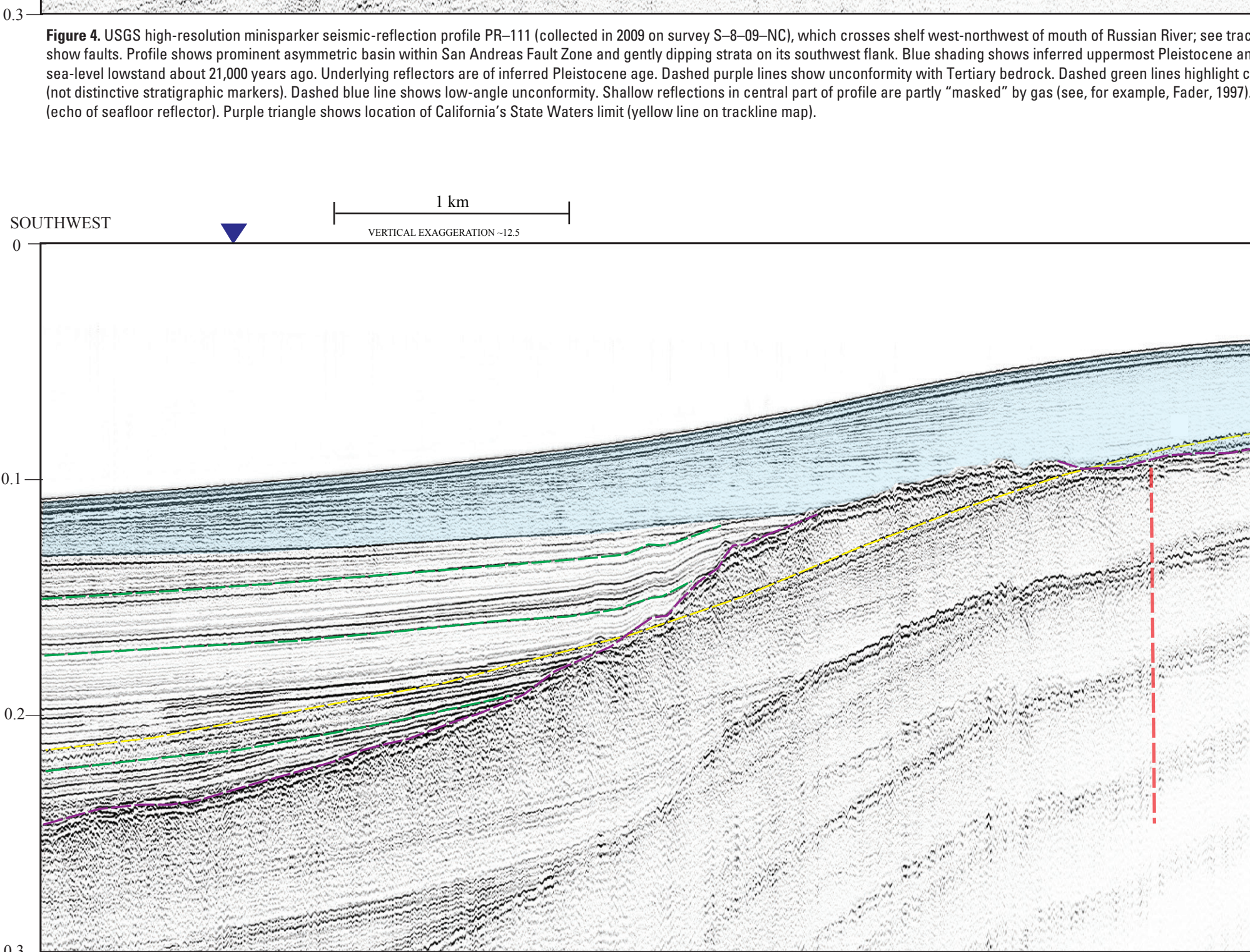
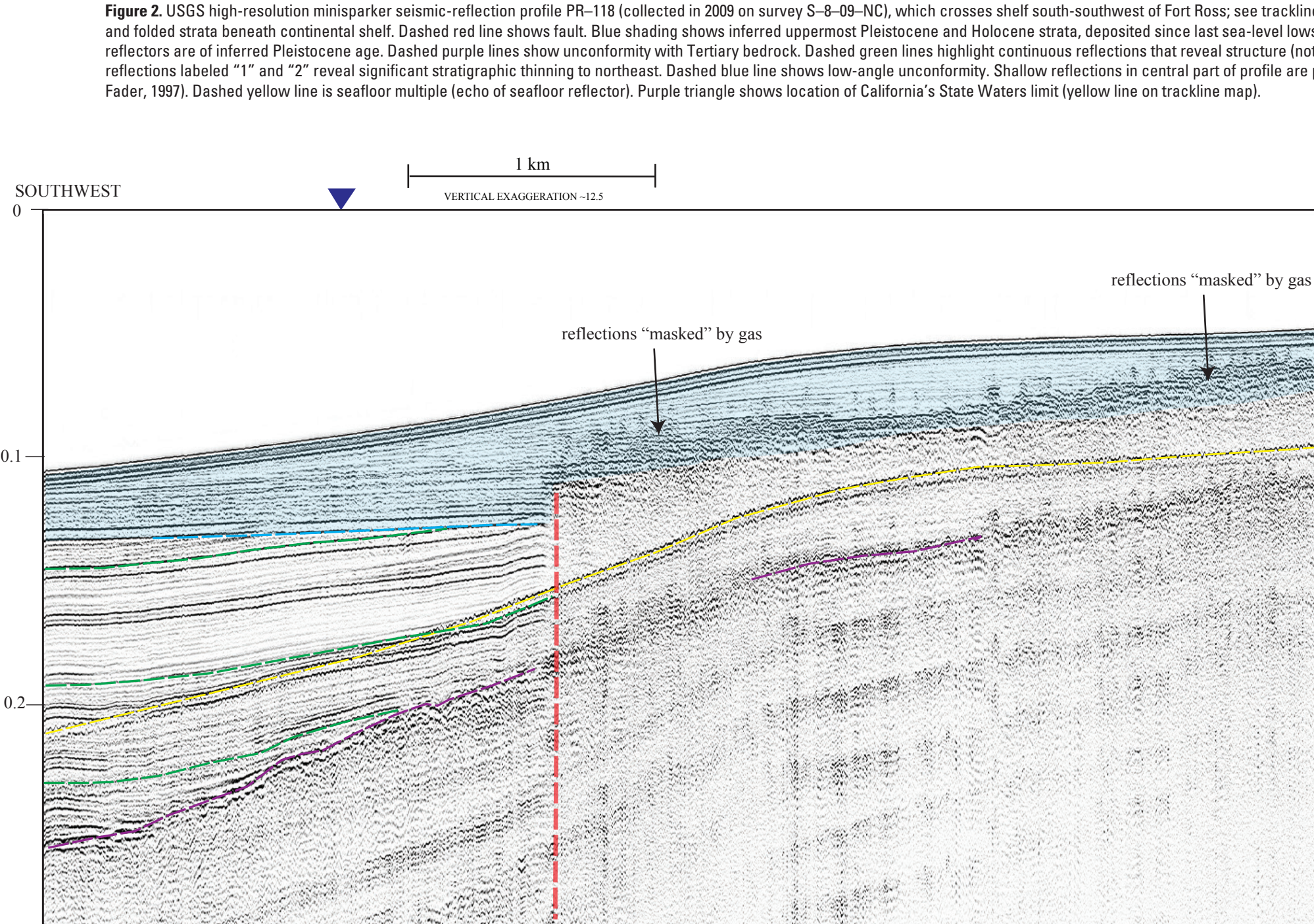
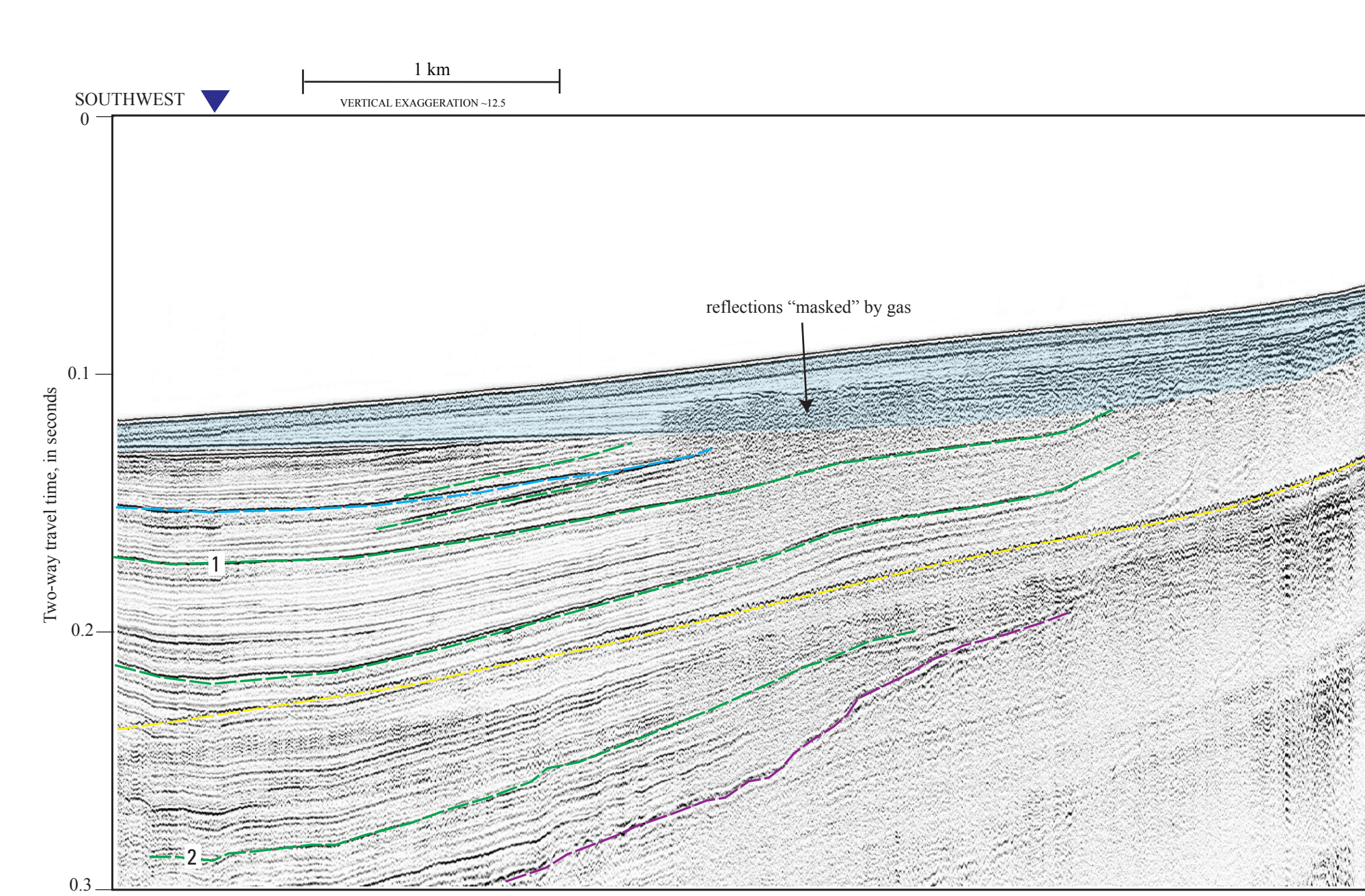
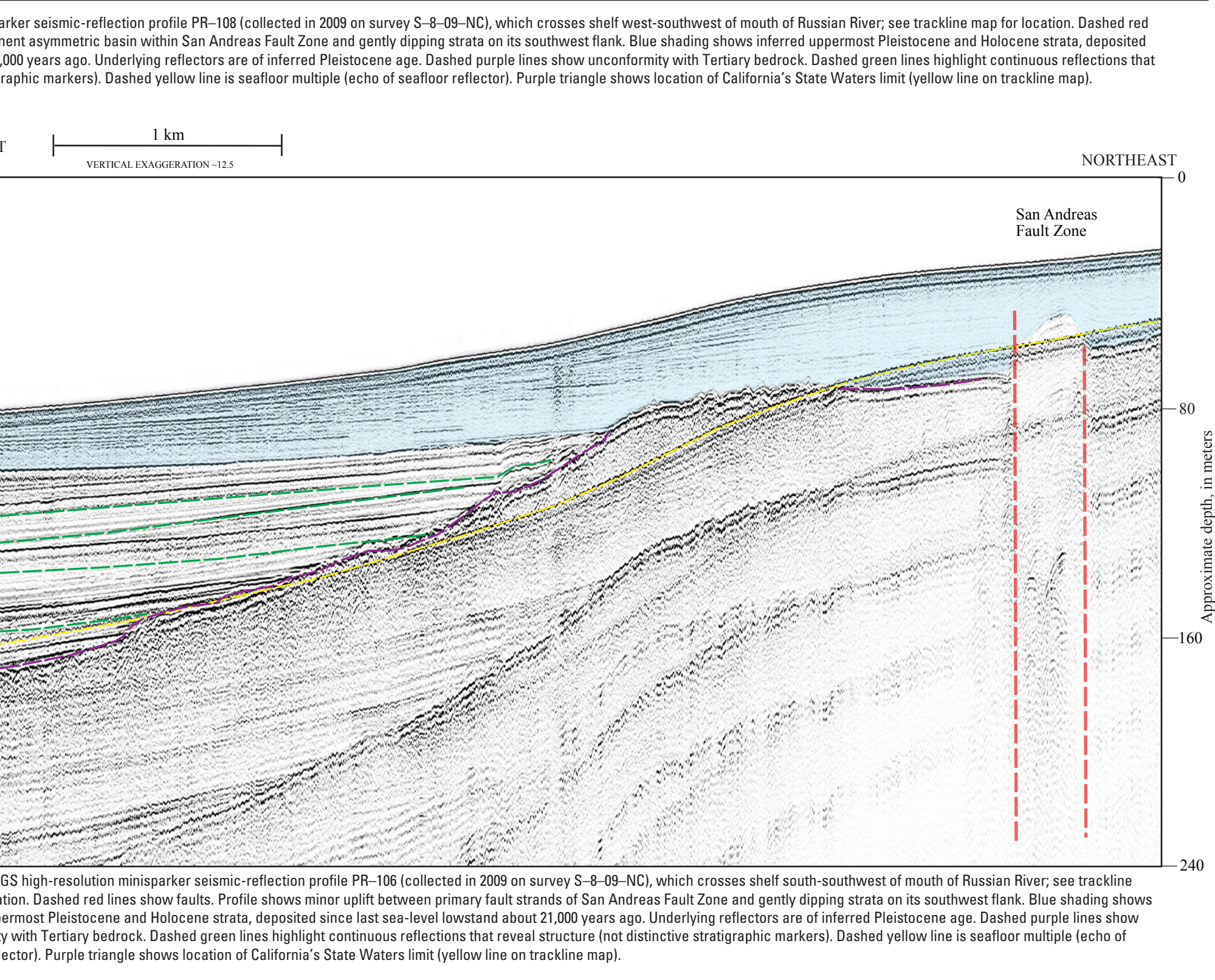
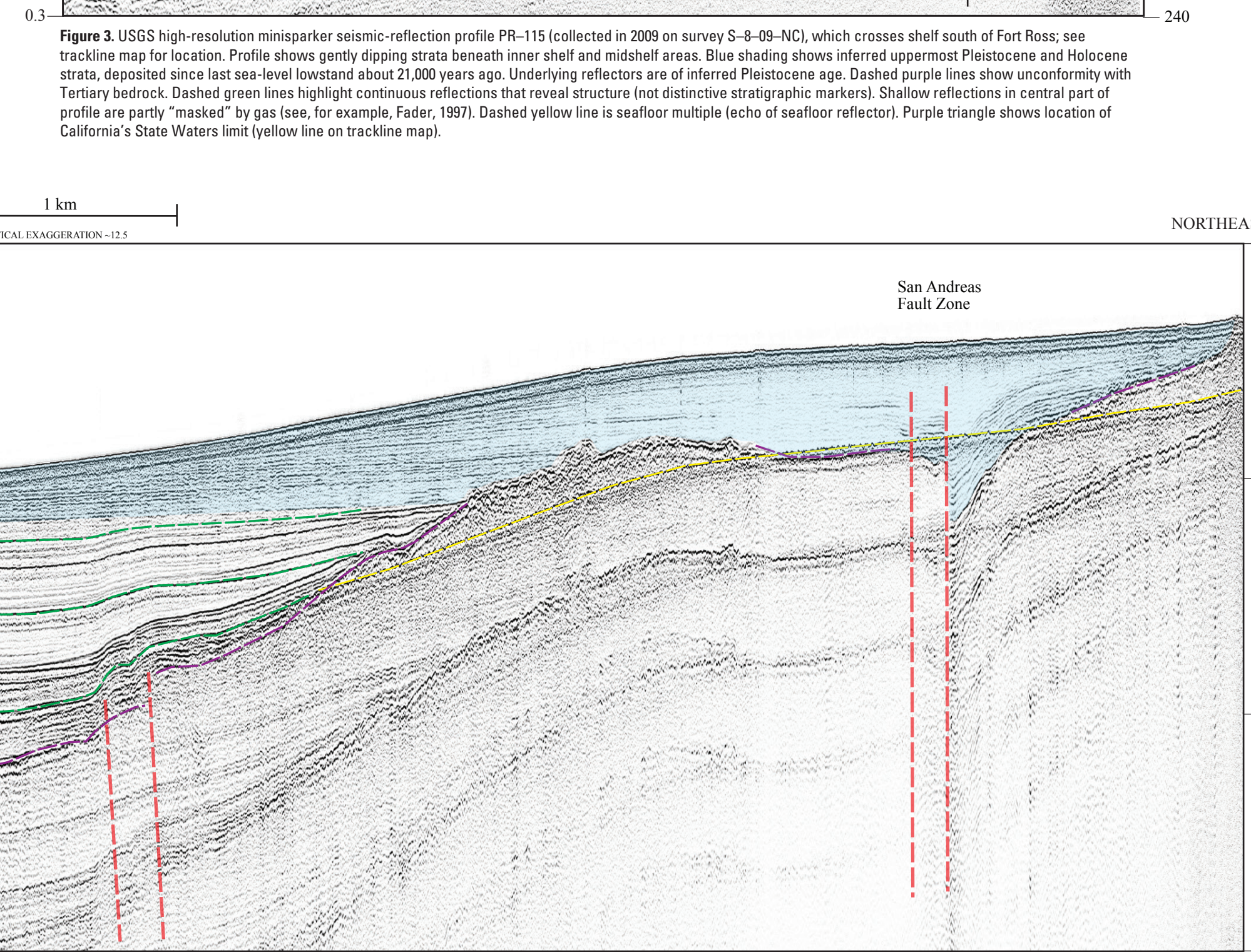
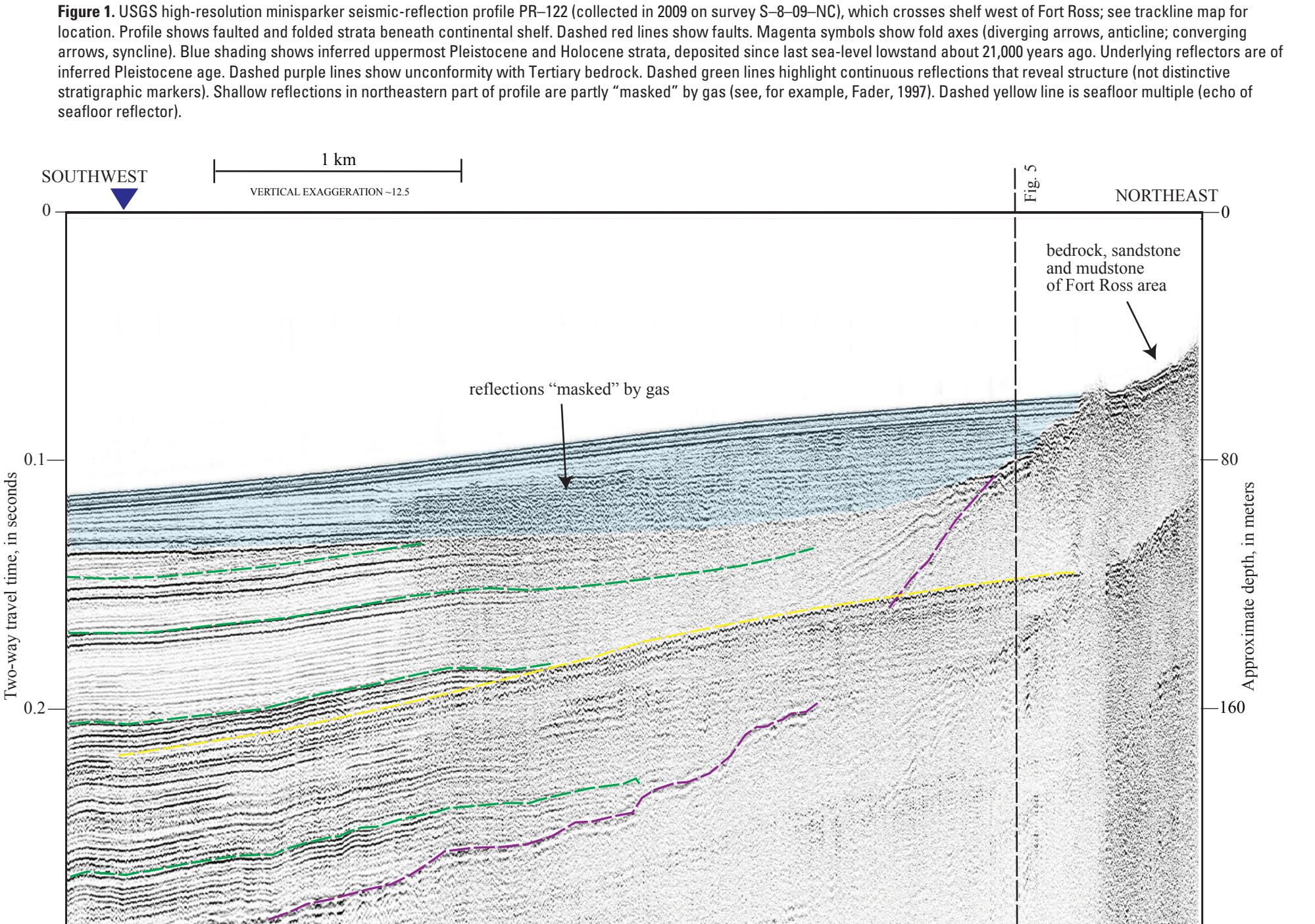
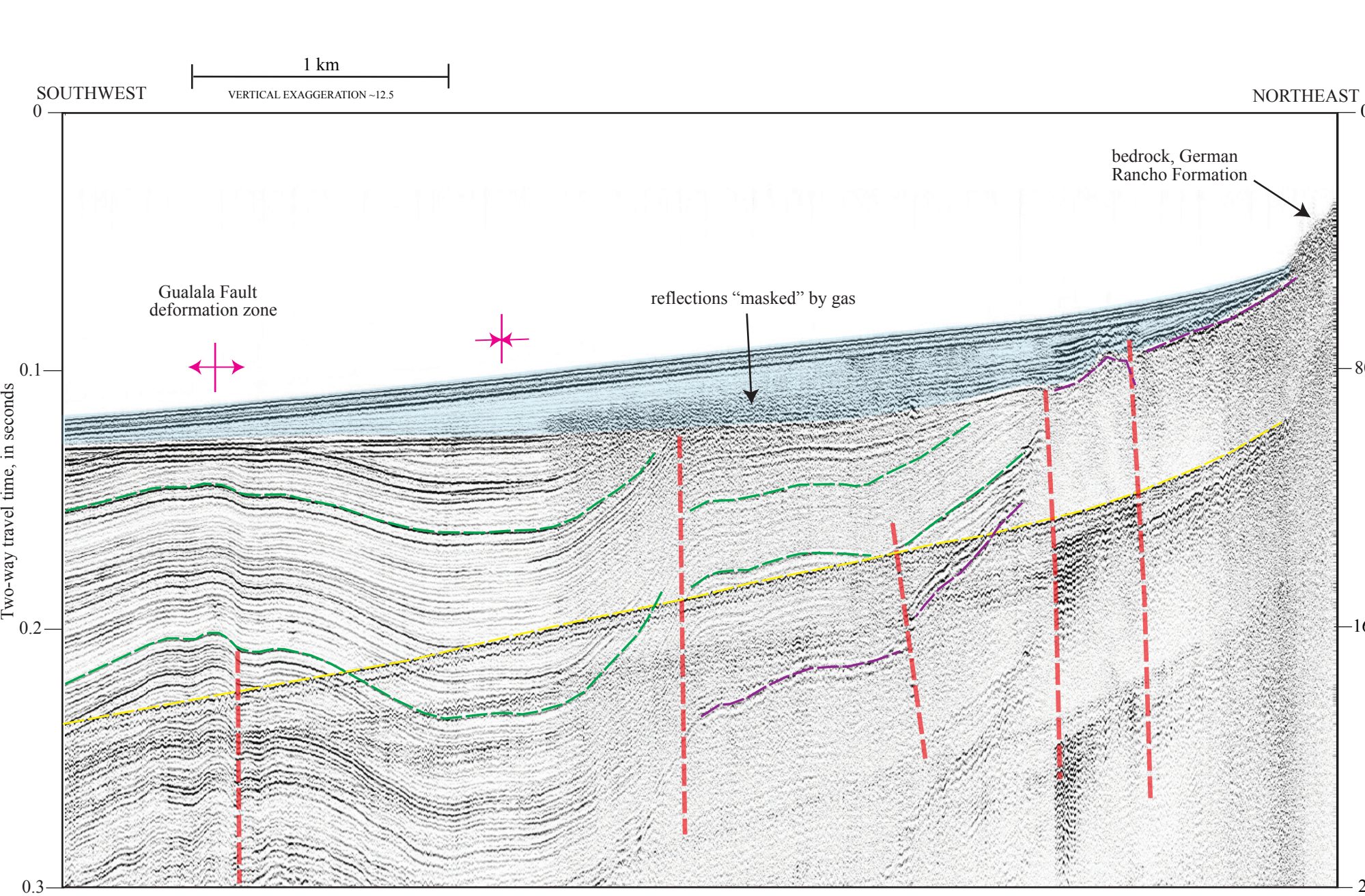
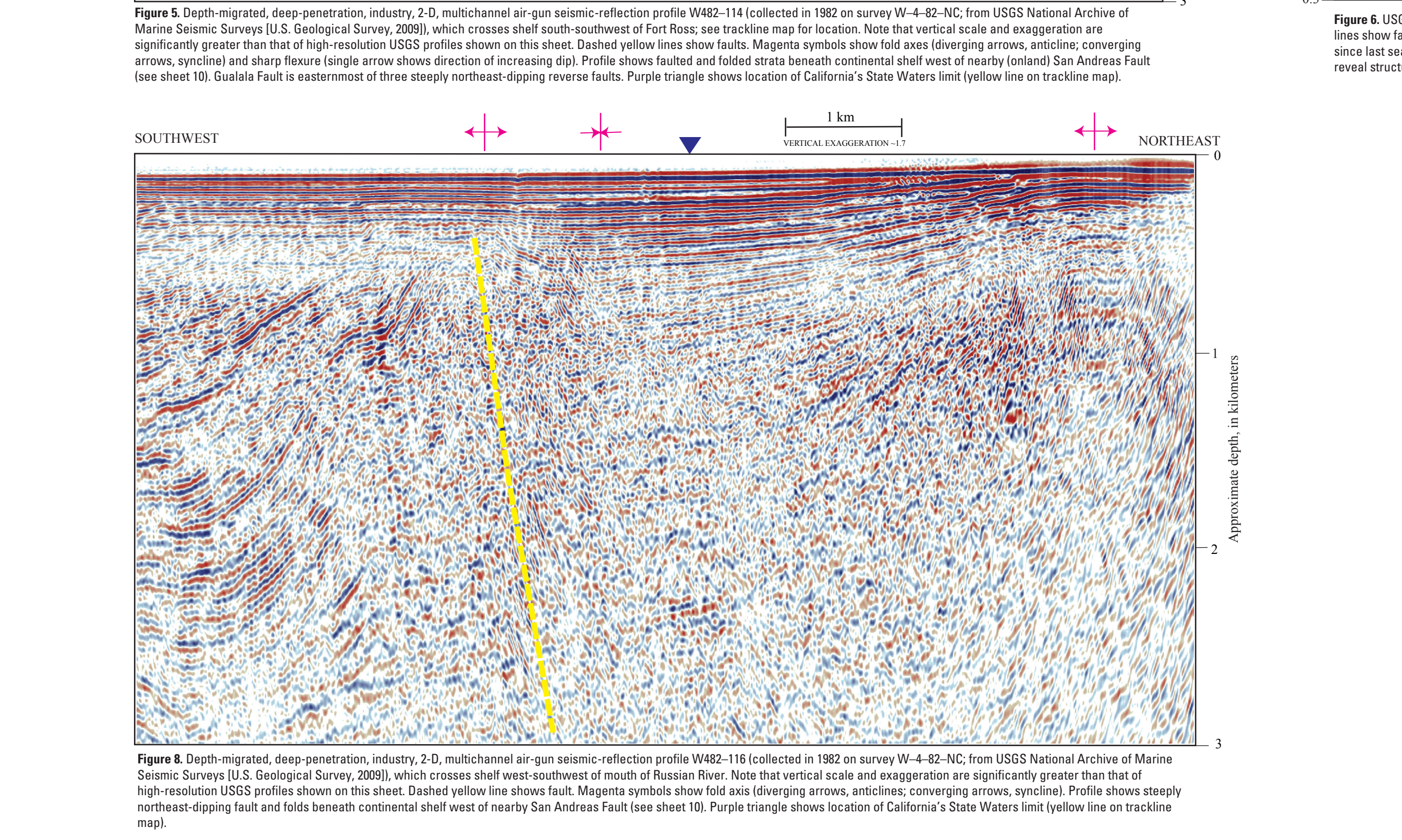
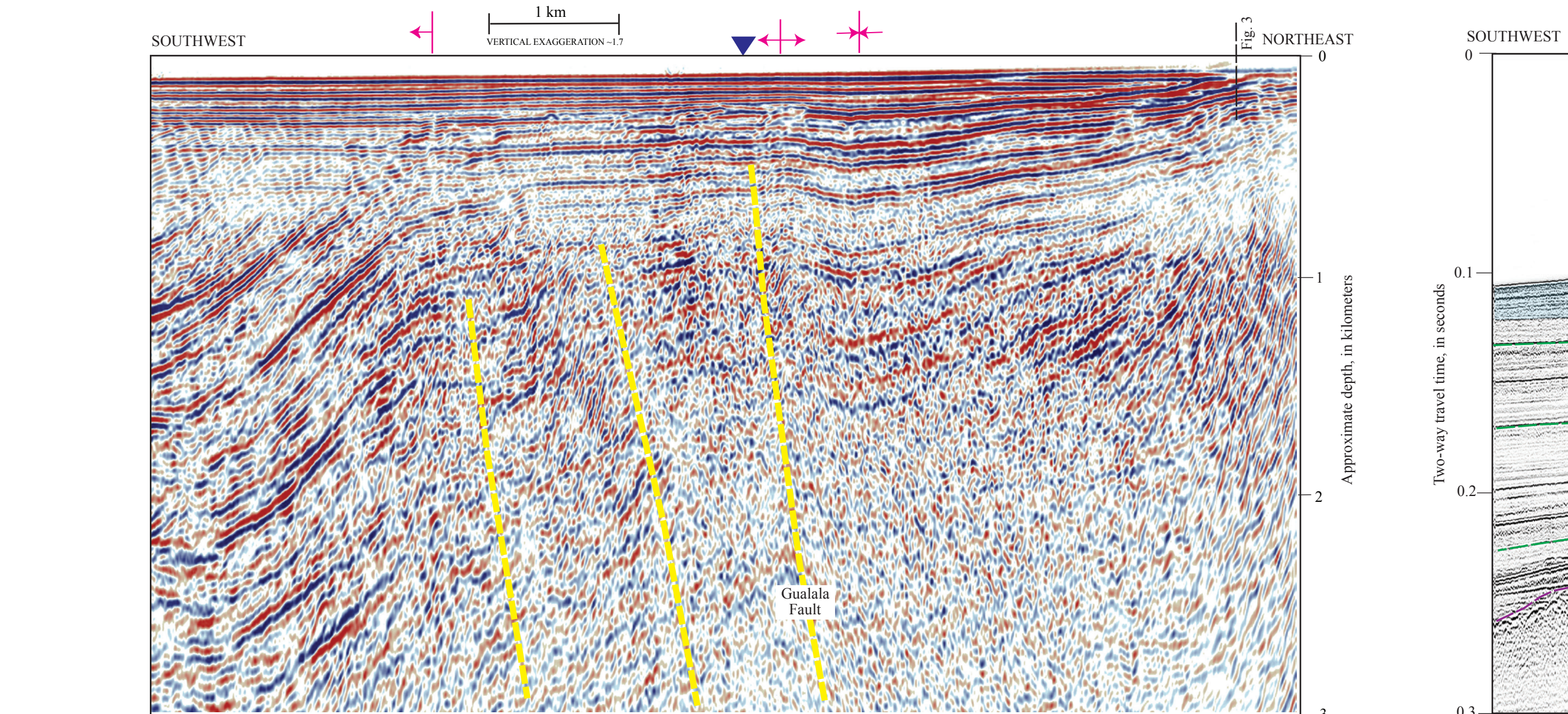


Seafloor elevation data from National Oceanic and Atmospheric Administration's Digital Coast Inventory of the Pacific Ocean (DOI/NOAA) and the U.S. Geological Survey's National Elevation Dataset (available at <http://ned.scripps.edu>). Offshore elevation control bathymetry from map sheet 10 of this report. California's State Waters limit from NOAA Office of Coast Survey. Source: Transverse Mercator projection, Zone 10N. NOT INTENDED FOR NAVIGATIONAL USE.

GIS database and digital cartography by Peter Derrall and Jaylene R. Farnard. Manuscript approved for publication November 5, 2015.



This map sheet shows seismic-reflection profiles from surveys of the Offshore of Fort Ross map area, providing imagery of the subsurface geology. The seismic-reflection profiles provide the data for interpreting subsurface stratigraphy, sediment thickness, and geologic structure (see sheets 9, 10 of this report).

The north half of the Offshore of Fort Ross map area is characterized by nearshore outcrops of Tertiary sedimentary rocks (see sheet 10 of this report). The nearshore zone and inner shelf (to the water depths of about 50 m) typically dip gently seaward (about 1.5° to 5.7°), whereas the middle shelf (about 50 to 85 m) is relatively flat (about 0.4°). In contrast, the nearshore to middle shelf area in the south half of the map area has a more uniform dip, about 0.45° to water depths of about 30 m and about 0.65° to 0.9° at water depths from 30 to 100 m. The south half of the map area has directly offshore of the Russian River, and this subsurface decrease in slope is caused by increased sedimentation and the resulting increase in sediment thickness (see Map 10 on sheet 9) in this wave-dominated, deltaic setting.

Shallow marine and shelf sediments were deposited in the last about 21,000 years during the sea-level rise that followed the last major lowstand associated with the Last Glacial Maximum (LGM) (Lambek and Chappell, 2001). Sea level was about 125 m lower during the LGM, at which time the Offshore of Fort Ross map area was emergent, and the shoreline was about 20 km west of its present location. The post-LGM sea-level rise was rapid (about 11 m per thousand years) until about 7,000 years ago, when it slowed considerably to about 1 m per thousand years (Stanford and others, 2011).

The sediments deposited during the post-LGM sea-level rise (the rapid transgression and highstand) are shaded blue in the high-resolution seismic-reflection profiles (Figs. 1, 2, 3, 4, 6, 7, 9, 10, 11), and their thickness is shown on sheet 9 (Map R, D). This post-LGM stratigraphic unit is characterized by relatively low-amplitude, low-to-high-frequency, parallel to divergent reflections that are continuous to moderately continuous (terminology from Michum and others, 1973). The contact with underlying units is an deep transgressive surface of erosion commonly marked by minor channeling and a common upward change to lower amplitude, more diffuse reflections.

Strata beneath the post-LGM unit (which overlies the Tertiary basement rocks) are represented in seismic-reflection profiles (Figs. 1, 2, 3, 4, 6, 7, 9, 10, 11) by low- to high-amplitude, high-frequency, parallel to subparallel, continuous reflections. Reflections commonly are flat to gently folded and typically have dips of 0° to 2° to a maximum (in the northern part of the map area) of about 5° (that dips may appear steeper on the profiles because of the 12.5:1 vertical exaggeration). The upper contact with the post-LGM unit ranges from angular to where the lower unit has been folded to parallel or subparallel. These strata are inferred to be Pleistocene in age (marine isotope stage 3 and older; Wolfbeck and others, 2002) because of their position with the post-LGM unit; in addition, their basins can be traced continuously, along with other USGS data from cruise S-8-09-NC), to the Quaternary sections penetrated by Shell Oil Company offshore well P-027-1 (15 km south of the map area; Heck and others, 1999). Similar to the overlying post-LGM deposits, these inferred Pleistocene strata are wave-eroded deltaic and shelf sediments derived primarily from the Russian River. Reflections within this interval are locally obscured by interstitial gas within the sediment (see, for example, Figs. 1, 2, 3, 4, 11). This effect has been referred to as "gas blanking," "acoustic turbidity," or "acoustic masking" (Fader, 1997). The gas scatters or attenuates the acoustic energy from the seismic-reflection-profiling system, inhibiting penetration of strata.

The map area is cut by the San Andreas Fault Zone (Figs. 4, 6, 7, 9, 10, 11; see also sheet 10). West of the San Andreas Fault, bedrock exposed above the coast (onshore and offshore) consists of the Palaeozoic and Cenozoic German Rancho Formation (Elder, 1968) and the lower Miocene sandstone and mudstone of Fort Ross area (see sheet 10). East of the San Andreas Fault, coastal bedrock outcrops consist of diverse Franciscan Complex, Franciscan, and Eocene rocks of the Franciscan Complex. The bedrock appears massive and reflections in low-resolution seismic-reflection data (see, for example, Figs. 2, 4, 6, 7, 9, 10), and it forms the acoustic basement for overlying Quaternary sediments. On the higher energy, lower resolution seismic profiles (Figs. 5, 8), bedrock west of the San Andreas Fault is inferred to be Tertiary sedimentary rocks characterized by low- to high-amplitude, parallel to divergent, continuous reflections.

The San Andreas Fault cuts through the Offshore of Fort Ross map area, enclosing the shoreline a few kilometers south of Fort Ross (see sheet 10). North of Fort Ross, the San Andreas Fault forms a prominent topographic high in low coastal hills. Geologic studies in the onshore area suggest a slip rate of 17 to 24 mm/y (U.S. Geological Survey and California Geological Survey, 2010). South of Fort Ross, the San Andreas Fault extends across the wave-dominated Russian River delta. The San Andreas Fault and other faults are identified on the seismic-reflection profiles on the basis of the shape, truncation or warping of reflections and/or the juxtaposition of reflection peaks that have differing seismic parameters, such as reflection presence, amplitude, frequency, geometry, continuity, and vertical sequence. The mapping reveals a 200- to 500-m-wide zone typically characterized by one to two primary fault strands (see sheet 10).

The map sheet shows six profiles that transect the San Andreas Fault (Figs. 4, 6, 7, 9, 10, 11), which illustrate the complex geometry within the fault zone. The northernmost three of these six profiles (Figs. 4, 6, 7) show prominent, asymmetric, intra-fault-zone basins (about 15 to 20 m deep) filled with post-LGM sediment, which probably represent subsidence and fort erosion within the fault zone and which may have captured the Russian River channel during the LGM sea-level lowstand. In contrast, two profiles (Figs. 9, 10), acquired 1 and 2 km south of the profile shown in figure 7, reveal gentle split between the two primary fault strands within the San Andreas Fault Zone. The fault zone has a gentle about 2.1 clockwise, extensional bend between the onshore and offshore parts of the zone, and this fault-zone bend is an inferred contact on local intra-fault-zone morphology (see, for example, Johnson and Watt, 2012).

The northeast-west of the San Andreas Fault in most of the Offshore of Fort Ross map area is relatively simple. The bedrock surface dips offshore about 1° to 2°, and it is overlain by an outward- and southward-dipping wedge of 1.5-m-thick reflections of inferred late Pleistocene age.

Except for the profiles in figures 5 and 8, all profiles displayed on this map sheet were collected in 2009 on USGS Geological Survey (USGS) cruise S-8-09-NC. The single-channel seismic-reflection data were acquired using the SGG 2Mille minisepair, which used a 500-kHz high-swing electrical shaver (fired 1.5 times per second), which, at normal sweep speeds of 4 to 4.5 m/s, would give a 2-m data trace every 0.5 to 2.0 meters. The data were digitally recorded in standard SEG-Y 12-bit floating-point format, using PC-based Triton Substation Logger (SLL) software that merges seismic-reflection data with differential GPS-acquired data. After the survey, a short-window (20 m) automatic gain control (AGC) was applied to the data, which was applied to the data with a 100- to 1,000-Hz bandpass filter and a 3-dB correction that uses an automatic seafloor-detection window (averaged over 30 m of lateral distance covered). These high-resolution data can resolve geologic features that are a few meters thick, down to subsection depths of about 400 m.

Figures 5 and 8 show deep-penetration, depth-migrated, multichannel seismic-reflection profiles collected in 1982 by WesternGeo on cruise W-4-82-NC. These profiles and other similar data were collected in many areas offshore of California in the 1970s and 1980s when these areas were considered a frontier for oil and gas exploration. Much of these data have been publicly released and are now archived at the USGS National Archive of Marine Seismic Surveys (U.S. Geological Survey, 2009). These data were acquired using a large-volume air-gun source that has a frequency range of 1 to 40 Hz and recorded with a multichannel hydrophone streamer about 2 km long. Shot spacing was about 30 m. These data can resolve geologic features that are 20 to 30 m thick, down to subsection depths of about 4 km.

REFERENCES CITED

Elder, W.P., 1968, Geology and tectonics of the Gualala Block, northern California: Society of Economic Paleontologists and Mineralogists, Pacific Section, Book 84, 222 p.

Fader, G.R.J., 1997, The effects of shallow gas on seismic reflection profiles, in Davies, T.A., Bell, T., Cooper, A.K., Josephson, H., Poljak, L., Solheim, A., Stokes, M.S., and Stravers, J.A., eds., Glaciated continental margins—An atlas of acoustic images: London, Chapman and Hall, p. 29-39.

Heck, R.G., Edwards, E.B., Kroon, J.D., Jr., and Willingham, C.R., 1990, Petroleum potential of the offshore outer Santa Cruz and Bodega basins, California, in Garrison, T.L., Green, H.G., Hicks, K.K., Weber, G.E., and Wright, T.L., eds., Geology and tectonics of the central California coastal region, San Francisco to Monterey, American Association of Petroleum Geologists, Pacific Section, Bulletin G167, p. 143-164.

Johnson, S.V., and Watt, J.E., 2012, Influence of fault trend, bends, and convergence on shallow structure and geomorphology of the Hogri strike-slip fault, offshore central California: Geosphere, v. 8, no. 6, p. 25, doi:10.1306/GS0803.12.

Lambek, K., and Chappell, J., 2001, Sea level change through the last glacial cycle: Science, v. 292, p. 679-686, doi:10.1126/science.1105449.

Michum, R.M., Jr., Vail, P.R., and Sangree, J.B., 1977, Seismic stratigraphy and global changes of sea level, part 6—Stratigraphic interpretation of seismic reflection patterns in depositional sequences, in Payton, F.E., ed., Seismic stratigraphy—Applications to hydrocarbon exploration: Tulsa, Oklahoma, American Association of Petroleum Geologists, p. 117-133.

Stanford, J.D., Homrighausen, R., Robling, E.J., Chalmon, P.G., Medina-Fitzke, M., and Lessor, A.J., 2011, Sea-level probability for the last deglaciation—A statistical analysis of ice-sheet records, Global and Planetary Change, v. 79, p. 193-200, doi:10.1016/j.gloplacha.2010.11.002.

U.S. Geological Survey, 2009, National Archive of Marine Seismic Surveys: U.S. Geological Survey database, available at <http://nams.usgs.gov/NAMSS/>.

U.S. Geological Survey and California Geological Survey, 2010, Quaternary fault and fold database of the United States: U.S. Geological Survey database, accessed April 5, 2014, at <http://earthquake.usgs.gov/faults/qa/qa/>.

Wolfbeck, C., Labeyrie, L., Michel, E., Duplessy, J.C., McManus, J.F., Lambeck, K., Balbon, E., and Labracherie, M., 2002, Sea-level and deep-water temperature changes derived from benthic foraminifera isotopic records, Quaternary Science Reviews, v. 21, p. 295-305.

